A Journal of the Gesellschaft Deutscher Chemiker

Angewandte International Edition Chemie

GDCh

www.angewandte.org

Accepted Article

Title: A Permselective CeOx Coating Improves the Stability of Oxygen Evolution Electrocatalysts

Authors: Keisuke Obata and Kazuhiro Takanabe

To be cited as: *Angew. Chem. Int. Ed.* 10.1002/anie.201712121
Angew. Chem. 10.1002/ange.201712121

Link to VoR: http://dx.doi.org/10.1002/anie.201712121
http://dx.doi.org/10.1002/ange.201712121

WILEY-VCH

10.1002/anie.201712121

WILEY-VCH

COMMUNICATION

A Permselective CeO_x Coating Improves the Stability of Oxygen Evolution Electrocatalysts

Keisuke Obata,[a] and Kazuhiro Takanabe*[a]

Abstract: Highly active $NiFeO_x$ electrocatalysts for the oxygen evolution reaction (OER) suffer gradual deactivation with time due to the loss of Fe species from the active sites into solution during catalysis. Here, we describe the anodic deposition of a CeO_x layer that prevents the loss of such Fe species from the OER catalysts, achieving a highly stable performance. The CeO_x layer does not affect the OER activity of the catalyst underneath but exhibits unique permselectivity, allowing the permeation of OH^- and O_2 through while preventing the diffusion of redox ions through the layer to function as a selective O_2-evolving electrode. The use of such permselective protective layer provides a new strategy for improving the durability of electrocatalysts.

Hydrogen is an energy carrier that can effectively store intermittent energy generated by renewable energy sources, such as solar and wind power. Many techniques, such as water electrolysis and photoelectrochemical water splitting, have been studied for the generation of hydrogen and oxygen from water. Unlike the hydrogen evolution reaction (HER) conducted on the cathodic side, the anodic oxygen evolution reaction (OER) is a kinetically sluggish reaction, requiring a substantial overpotential. Highly active, durable and cost-effective electrocatalysts for OER are desired for the development of an efficient water splitting device. $NiFeO_x$ is one of the most active electrocatalysts for OER in alkaline conditions, and while it is known that Fe plays a critical role in the improved activity,[1] the origin of the enhancement of the OER kinetics by Fe doping is still under debate. Although many studies have been devoted to decreasing the overpotential via the development of an LDH structure,[2] compositional control,[3] or deposition on a conductive support with high surface area,[4] few reports have discussed the stability under harsh oxidative conditions.[5] Gorlin et al. reported a significant overpotential increase (approximately 30 mV) on $Ni_{0.65}Fe_{0.35}O_x$ over 20 h during a constant current electrolysis at 10 mA cm^{-2}.[5c] Speck et al. observed that the iron content in the $Ni_{0.5}Fe_{0.5}O_x$ catalyst decreased from the loss of FeO_4^{2-} species after the overpotential increased by approximately 200 mV during the stability test at 200 mA cm^{-2} for 24 h.[5d] FeOOH is also known to dissolve as FeO_4^{2-} during OER in alkaline solutions.[6] We address this stability issue of an active OER electrode by coating the electrode with a protective thin layer that allows the evolved O_2 to penetrate, without losing dissolved ion species from the active surface into the solution. Herein, we report that an anodically deposited CeO_x layer successfully realizes this unique permselectivity that results in a highly stable performance of the $NiFeO_x$ catalyst.

$NiFeO_x$ was prepared on a Au substrate by conventional cathodic deposition[7] and was used as the base electrode. The CeO_x layer was formed on the $NiFeO_x$ by applying a constant anodic potential of 1.7 V vs. the reversible hydrogen electrode (RHE) in the deposition solution containing 0.4 M cerium nitrate and 0.4 M ammonium acetate (pH = 7).[8] The optimal deposition time was found to be 6 h (vide infra). In the deposition solution, Ce^{3+} is oxidized and precipitates on the anode due to the lower solubility of Ce^{4+} compared to Ce^{3+}.[8] Because $Ni(OH)_2$ becomes conductive only after oxidation to NiOOH,[9] we applied a more anodic potential (1.7 V vs. RHE) than that for the oxidization of Ce^{3+} (1.0 V vs. RHE) to deposit CeO_x on top of $NiFeO_x$ (Figure S1a and S1b), where oxygen is evolved. Ce^{3+} can also be oxidized by O_2 evolved from the anode, making the Ce deposition process rather complex.[10] Using inductively coupled plasma (ICP) (Table S1), the total amount of deposited Ce was measured to be 1.9±0.2 μmol cm^{-2}. The total charge passed during the deposition was 13±1 C cm^{-2}, corresponding to 150±11 μmol cm^{-2} of electrons (Figure S1c). Therefore, only less than 10% of total charge was utilized for the deposition process.

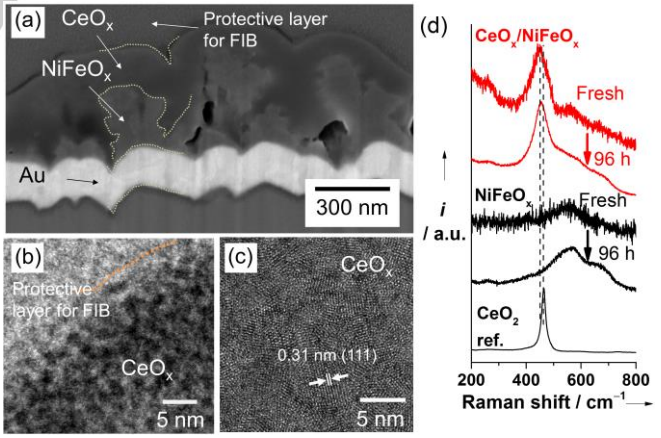

Figure 1. (a) Cross-sectional (milled by focused ion beam (FIB)) SEM images of CeO_x-coated $NiFeO_x$. (b) (c) high resolution TEM images of CeO_x layer. (d) Raman spectra of bare and CeO_x-coated $NiFeO_x$ electrode and commercial CeO_2. Raman spectra were obtained before and after the stability test at 20 mA cm^{-2} for 96 h.

Top-view scanning electron microscopy (SEM) images of bare $NiFeO_x$ and the CeO_x-coated $NiFeO_x$ electrodes are shown in Figure S2a and S2b, respectively, and the cross-sectional

[a] K. Obata, Prof. K. Takanabe
King Abdullah University of Science and Technology (KAUST)
KAUST Catalysis Center (KCC) and Physical Sciences and Engineering Division (PSE)
4700 KAUST, Thuwal, 23955-6900, Saudi Arabia
E-mail: kazuhiro.takanabe@kaust.edu.sa

Supporting information for this article is given via a link at the end of the document.

10.1002/anie.201712121

image of the latter is shown in Figure 1a. It can be seen that the cathodically deposited $NiFeO_x$ had a coarse structure on the Au substrate, and the CeO_x layer was uniformly formed with a thickness in the 100 - 200 nm range on top of the $NiFeO_x$. Transmission electron microscopy (TEM) image of CeO_x layer revealed that approximately 5 nm of nanoparticles aggregated to form the layer consisting apparent voids between them (Figure 1b). The CeO_x material at the $NiFeO_x$ surface seems to be more porous than the bulk layer (Figure S2d) and some lattice fringes suggest the existence of ultrafine crystalline structure of CeO_2, which is confirmed by selected-area electron diffraction (SAED), forming its aggregated layer (Figure 1c and S2e). Raman spectra show an Oī Ceī O vibration at approximately 450 $cm^{ī 1}$ with the broad Niī O vibration peak[11] from $Ni(OH)_2$ at approximately 560 $cm^{ī 1}$ (Figure 1d). When compared to commercial crystalline CeO_2, the Oī Ceī O vibration was shifted toward lower wavenumber values, and the peak shape became broader. This difference can be due to the particle size or coexistence of Ce^{3+}.[12] The XRD diffraction pattern did not show any peaks from crystalline CeO_2 apparently because of fine crystalline particles (Figure S3). It showed a broad peak at approximately 25°, indicating the coexistence of the amorphous phase. XPS spectra of Ce 3d showed a multiplet splitting composed of Ce^{3+} and Ce^{4+},[13] indicating that Ce^{3+} precipitated together with Ce^{4+} (Figure S4a). O 1s spectra showed two main peaks at 529 eV and 532 eV, characteristic of oxide and hydroxide[13a,13b,14], respectively (Figure S4b).

Figure 2a shows a stability test of uncoated and CeO_x-coated $NiFeO_x$ at 20 mA $cm^{ī 2}$ in 1 M KOH. Uncoated $NiFeO_x$ reached 20 mA $cm^{ī 2}$ at 1.53 V vs. RHE in the beginning of the stability test, but the overpotential increased with time by more than 60 mV over 96 h. On the other hand, CeO_x-coated $NiFeO_x$ maintained its overpotential for 96 h, while the potential to achieve 20 mA $cm^{ī 2}$ was similar to the uncoated $NiFeO_x$ at the initial stage. In the cyclic voltammogram (CV) measured immediately after the stability test (96 h), a slight recovery of the current toward OER was observed at the second cycle, without going back completely to the original current density measured prior to the stability test on the bare $NiFeO_x$ electrode (Figure 2b). It is often reported that a cathodic sweep or resting potential help to recover the current of deactivated $NiFeO_x$ to some extent,[5a,5b] but the reason for this still remains unclear. In contrast, although a slight increase of the overpotential (~10 mV) was observed during the stability test for CeO_x-coated $NiFeO_x$, by potential sweeping, the OER current recovered completely to the original value that was measured prior to the stability test (Figure 2b). This full recovery was in marked contrast to the behavior observed for the bare $NiFeO_x$ electrode. Importantly, the Tafel slope remained ~40 mV $dec^{ī 1}$ after the CeO_x deposition (Figure 2c), clearly suggesting that the CeO_x layer did not affect the reaction mechanism of $NiFeO_x$ toward OER.

Examination of the Raman spectra obtained after the stability test shows that a broad peak due to NiO[11a] appeared at approximately 670 $cm^{ī 1}$ on the bare and CeO_x-coated $NiFeO_x$ (Figure 1d). The Oī Ceī O vibration remained broad and shifted to lower wavenumber compared to commercial CeO_2. XPS spectra also showed that the coexistence of Ce^{3+} and Ce^{4+} was retained, along with the coexistence of the oxide and hydroxide, after anodic polarization (Figure S4c and S4d). These results indicate that the CeO_x layer did not show a significant change in its crystal nature after the OER. From ICP measurement, the amount of Fe in the bare $NiFeO_x$ remained unchanged after stability test (Table S1) in contrast with the previous report observing content of Fe dropped from 50% to 25%.[5d] It is consistent with the claim in the literature that only limited amount of Fe was highly active sites[15] and those sites were lost, which could not be quantified by our ICP measurement. Alternatively, the amount of Ce remained unchanged after long current electrolysis, suggesting that CeO_x layer was not a sacrificial layer. Top-view SEM images of CeO_x-coated $NiFeO_x$ electrode after stability test also shows that CeO_x layer maintained similar morphology compared with that before the stability test (Figure S2b and S2c).

A comparison of the redox peaks of $Ni^{2+/3+}$ in the CVs measured before and after the stability test showed that the redox peaks exhibited a similar negative shift after anodic polarization on bare and CeO_x-coated $NiFeO_x$ (Figure S6) despite their different stabilities. This indicates that the redox peak position of $Ni^{2+/3+}$ does not reflect the OER activity, in agreement with a previous report.[15b] Impedance spectra of the bare and CeO_x-coated $NiFeO_x$ electrodes show a single semicircle that arises from the parallel connection of the charge transfer resistance (R_{CT}) toward OER and the double layer capacitance (C_{dl}) (Figure S7a and S7c). The corresponding transition appeared at approximately 100 Hz in the Bode plot (Figure S7b). A thick oxide film was often reported to show an additional semicircle in the Nyquist plot and the corresponding peak of the phase and step of log|Z| at approximately 1 kHz in the Bode plot. This additional semicircle is assigned to the parallel connection of the resistance (R_f) and capacitance (C_f) from the oxide film[16] (Figure S7d) and induces a potential drop through the oxide film. CeO_x-coated $NiFeO_x$ did not show any other observable semicircle, which also implies that the CeO_x layer itself did not cause a potential loss through the layer in alkaline conditions.

An electrode with CeO_x directly deposited on Au without $NiFeO_x$ did not exhibit any appreciable current at ~1.5 V vs. RHE, confirming that CeO_x itself is not relatively active for OER (Figure S8). When the deposition process was conducted in the absence of the Ce^{3+} precursor, the stability of the $NiFeO_x$ was not improved, also confirming that the deposition of the CeO_x layer is essential for obtaining a stable OER performance (Figure S9), i.e., either acetate or ammonium ions in the deposition solution alone did not contribute to the improved stability.

Another possibility to cause improved stability is that the Ce species alters the nature of $NiFeO_x$. Doping of Ce into the Ni-based catalyst is reported to improve the kinetics of OER and 3-5 nm of segregated CeO_2 was reported after electrochemical measurements even though the contribution of CeO_2 to the improved kinetics is still under investigation.[17] Therefore, different compositions of $NiFeCeO_x$ electrodes were also prepared by adding $Ce(NO)_3$ into the solution for cathodic deposition of oxide catalysts. The compositions of deposition solutions and deposited electrocatalysts are shown in Table S2, demonstrating the successful incorporation of the Ce species into $NiFeO_x$. $Ni_{0.84}Fe_{0.14}Ce_{0.02}O_x$ indeed exhibited improved OER performance (both onset and current) compared to $NiFeO_x$ without Ce incorporation (Figure S10a and S10b). The introduction of an additional CeO_x layer did not alter the initial OER performance but largely improved the stability (Figure S10c).

10.1002/anie.201712121

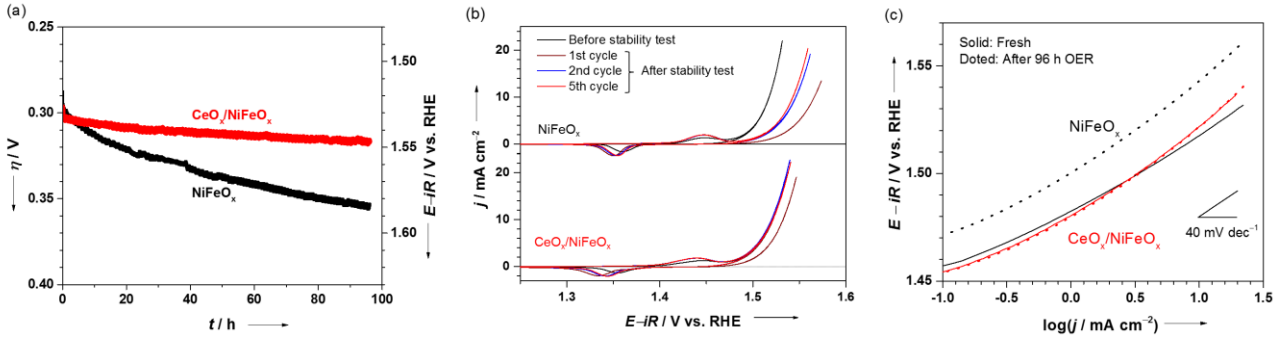

Figure 2. (a) Electrocatalytic stability test by controlled current electrolysis at 20 mA cm^{-2}. Cyclic voltammograms of (b) bare $NiFeO_x$ and (c) $CeO_x/NiFeO_x$ electrodes before and after the stability test. (d) Tafel plot taken from cyclic voltammograms. Scans (20 mV s^{-1}) in the negative direction are shown. All the measurements were conducted in purified 1 M KOH at 298 K with O_2 bubbling.

In an alternative approach, the deposition of CeO_x was also conducted on CoO_x nanoparticles (SEM images are shown in Figure S5).[18] An accelerated stability test was performed by cyclic voltammetry in 0.5 M phosphate buffer solution (pH = 7) (Figure S15). Bare CoO_x showed a drastic decrease of the current and a positive shift of the onset potential with potential cycles that were attributed to the gradual loss of the Co species from the electrode surface.[19] The CeO_x coating did not alter the initial onset, i.e., the electrocatalytic activity of CoO_x. These observations are attributed to the confinement introduced by the layer where the dissolved Co species is maintained within the layer, assisting self-healing.[20] Thus, the essential role of the additional CeO_x layer for the stability was confirmed to be universal regardless of the OER catalysts.

The permselectivity of the CeO_x layer in the presence of various kinds of reducing agents, which can be oxidized on $NiFeO_x$, was investigated by electrochemical measurements. Figure 3a shows representative cyclic voltammograms of the bare and CeO_x-coated $NiFeO_x$ electrodes in 1 M KOH with and without 0.2 M $K_4Fe(CN)_6$. In the alkaline solution with the ferrocyanide redox ions, bare $NiFeO_x$ displays the oxidation and reduction peaks of ferrocyanide and ferricyanide, which has the redox formal potential at 1.33 V vs. RHE in pH 14, followed by the redox peaks of $Ni^{2+/3+}$. On the other hand, CeO_x-coated $NiFeO_x$ does not show any redox peaks of the ferrocyanide ions, and only the redox peaks from $Ni^{2+/3+}$ as if ferrocyanide ions are absent were observed, implying that the CeO_x layer blocked the permeation and charge transfer of ferrocyanide. Then, CeO_x-coated $NiFeO_x$ electrodes with different deposition times were prepared and tested for the same experiment (Figure S11). Comparing the currents at 1.4 V vs. RHE where ferrocyanide oxidation contribution is obvious, CeO_x-coated $NiFeO_x$ with 2 h of deposition detected a higher current for the oxidation of ferrocyanide. This indicates that more than 4 h of deposition are necessary to obtain sufficient permselectivity. This permselectivity was also confirmed by gas quantification of O_2 during controlled current electrolysis at 10 mA cm^{-2} (Figure S12a). In the case of bare $NiFeO_x$, oxygen was not detected in the initial 3 h, indicating that the oxidation of the redox mediator dominated on the bare $NiFeO_x$ surface rather than OER. After 3 h of electrolysis, oxygen started to evolve only gradually due to the decreasing concentration of redox species during the electrolysis and resultant diffusion limitation of redox species. On the other hand, >90% of the faradaic efficiency to O_2 was maintained on $CeO_x/NiFeO_x$ after 7 h.

To further investigate the permselectivity of the CeO_x layer, Faradaic efficiencies of O_2 in the presence of different kinds of reducing agents, such as iodide, methanol, ethanol, isopropanol, lactate and malate, were further evaluated (Figure S12b-S12g) and are summarized in Figure 3b with the corresponding Stokes radii, which were estimated from the corresponding diffusion coefficients in aqueous solution.[21] In alkaline solutions, all reducing agents used are more thermodynamically preferred to be converted than OER.[22] Among different alcohols, bulkier *i*-PrOH reaction was more suppressed than smaller MeOH by the CeO_x layer. A clear improvement of selectivity toward O_2 was observed in the solution with redox anions rather than neutral alcohols. Notably, while lactate anion and isopropanol have similar Stokes radii, significant improvement for OER selectivity was obtained in the presence of lactate anion, suggesting that charges of reactants play a significant role to the permeation through the CeO_x layer. This trend suggests that diffusion of the reducing agents is impacted not only by their sizes but also by their charges. Since the isoelectronic point of CeO_2 is reported to be approximately 7,[23] the CeO_x layer should be negatively charged and repulse anions, resulting in the more effective suppression of the diffusion of the anion through the layer in alkaline conditions. Although OH^- ions are also negatively charged, the CeO_x layer electrodeposited by anodic polarization was reported to have a hydrous disordered structure,[24] which could contribute to the diffusion of OH^- to the $NiFeO_x$ catalyst underneath the layer.

The coating of the CeO_x layer can be applied to water splitting in the presence of Cl^- to improve the stability of the $NiFeO_x$ catalysts. The overpotential of $NiFeO_x$ increased by more than 60 mV in 6 h in the solution with 1 M KCl, while it increased by 30 mV in the solution without KCl (Figure S13). No oxidation of Cl^- was observed in alkaline conditions because the redox potential is reported to be 1.72 V vs. RHE,[25] which is higher than the observed potential. Cl^- appears to facilitate the deactivation of

10.1002/anie.201712121

$NiFeO_x$, as was also observed in a previous study,[25] even though the reason of the promoted degradation is not well-understood. On the other hand, the overpotential of CeO_x-coated $NiFeO_x$ increased only by 15 mV in 6 h, which was comparable to that for bare $NiFeO_x$ at the beginning of the stability test.

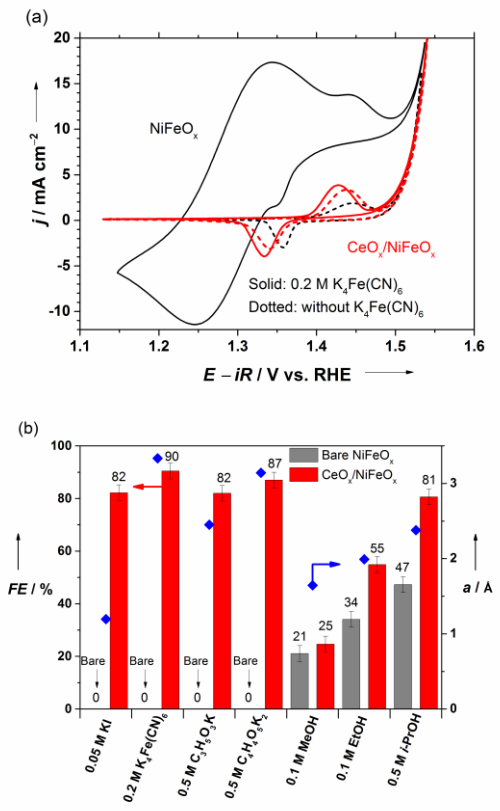

Figure 3. (a) Cyclic voltammograms for the bare and CeO_x-coated $NiFeO_x$ electrodes in 1 M KOH solution with and without 0.2 M $K_4Fe(CN)_6$ under Ar atmosphere (condition: 20 mV s^{-1}, 298 K). (b) Faradaic efficiency of O_2 during controlled current electrolysis at 10 mA cm^{-2} for the bare and CeO_x-coated $NiFeO_x$ electrode in 1 M KOH solution in the presence of different kinds of reducing agents with the corresponding Stokes radii.

Suppressed anion diffusion was also observed in near-neutral 0.5 M $K_{0.6}H_{2.4}BO_3$ solution (pH = 9.4). The overpotential toward OER increased drastically due to the deposition of CeO_x, while those in 1 M KOH for bare and CeO_x-coated $NiFeO_x$ were quite similar (Figure S14). In neutral pH (< 11), buffer anions are required to continuously remove the protons produced from water during OER because the insufficient amount of OH^- induces reactant switching from OH^- to water.[26] The increased overpotential due to the CeO_x layer also indicates that the presence of the CeO_x layer prevented the diffusion of the buffer anion, which unfortunately limits the applicability of CeO_x in buffered condition at least when the layer is thick.

Based on these results, the CeO_x layer is confirmed to show permselectivity, which prevents the detrimental redox species from diffusing through. Scheme 1 summarizes the permselective functionality of the CeO_x layer. In particular, the layer suppresses the diffusion of dissolved Fe species from catalyst to the electrolyte, resulting in the preservation of the active sites in $NiFeO_x$ during anodic polarization.

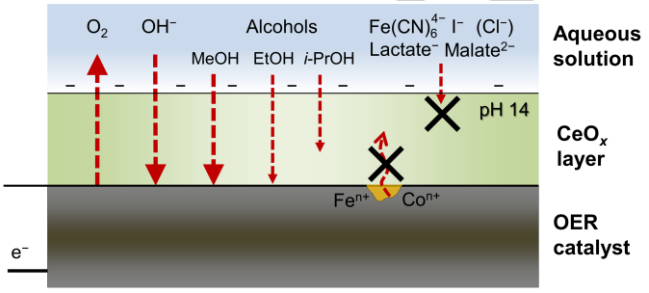

Scheme 1. Schematic image of the improved stability and selectivity achieved by the deposition of CeO_x on the OER catalyst.

In conclusion, we successfully developed a highly durable $NiFeO_x$ OER electrocatalyst by the anodic deposition of a CeO_x layer on it. The CeO_x consisted of a mixed oxide and hydroxide layer, which prevented the diffusion of redox ions while allowing OH^- and evolved O_2 to permeate through. The improved stability of the OER catalysts was attributed to permselectivity, which can regulate the diffusion of redox ions, such as iodide, ferrocyanide and dissolved metal ion species, between the electrolyte and OER catalysts. CeO_x protection is also applicable to other OER materials and obviously to corrosion inhibition without electrocatalysis, demonstrating the universality of the permselective function applicability. This finding demonstrates a promising novel approach for introducing an inorganic layer by anodic deposition for highly active and durable OER catalysts that operate in harsh oxidative conditions.

Acknowledgements

The research reported in this publication was supported by King Abdullah University of Science and Technology (KAUST). The authors appreciate the kind assistance of Dr. J. Bau at KAUST for TEM images.

Keywords: electrochemistry Åenergy conversion Å heterogeneous catalysis Åoxygen evolution Åwater splitting

[1] a) D. Friebel, M. W. Louie, M. Bajdich, K. E. Sanwald, Y. Cai, A. M. Wise, M.-J. Cheng, D. Sokaras, T.-C. Weng, R. Alonso-Mori, R. C. Davis, J. R. Bargar, J. K. Nørskov, A. Nilsson, A. T. Bell, *J. Am. Chem. Soc.* **2015**, *137*, 1305ī 1313; b) L. J. Enman, M. S. Burke, A. S. Batchellor, S. W. Boettcher, *ACS Catal.* **2016**, *6*, 2416ī 2423; c) H. S. Ahn, A. J. Bard, *J. Am. Chem. Soc.* **2016**, *138*, 313ī 318.

[2] a) M. Gong, Y. Li, H. Wang, Y. Liang, J. Z. Wu, J. Zhou, J. Wang, T. Regier, F. Wei, H. Dai, *J. Am. Chem. Soc*. **2013**, *135*, 8452ī 8455; b) Z. Lu, W. Xu, W. Zhu, Q. Yang, X. Lei, J. Liu, Y. Li, X. Sun, X. Duan, *Chem. Commun.* **2014**, *50*, 6479ī 6482; c) C. Wang, R. B. Moghaddam, M. J. Brett, S. H. Bergens, *ACS Sustainable Chem. Eng.* **2017**, *5*, 1106ī 1113.

[3] J. R. Swierk, S. Klaus, L. Trotochaud, A. T. Bell, T. D. Tilley, *J. Phys. Chem. C* **2015**, *119*, 19022ī 19029.

[4] a) X. Lu, C. Zhao, *Nat. Commun*. **2016**, *6*, 6616; b) E. Nurlaela, T. Shinagawa, M. Qureshi, D. S. Dhawale, K. Takanabe, *ACS Catal*. **2016**, *6*, 1713ï 1722.

[5] a) J. Luo, J.-H. Im, M. T. Mayer, M. Schreier, M. K. Nazeeruddin, N.-G. Park, S. D. Tilley, H. J. Fan, M. Grätzel, *Science* **2014**, *345*, 1593ï 1596; b) M. B. Stevens, L. J. Enman, A. S. Batchellor, M. R. Cosby, A. E. Vise, C. D. M. Trang, S. W. Boettcher, *Chem. Mater.* **2017**, *29*, 120ï 140; c) M. Gorlin, J. F. de Araújo, H. Schmies, D. Bernsmeier, S. Dresp, M. Gliech, Z. Jusys, P. Chernev, R. Kraehnert, H. Dau, P. Strasser, *J. Am. Chem. Soc.* **2017**, *139*, 2070ï 2082; d) F. D. Speck, K. E. Dettelbach, R. S. Sherbo, D. A. Salvatore, A. Huang, C. P. Berlinguette, *Chem.* **2017**, *2*, 590ï 597.

[6] S. Zou, M. S. Burke, M. G. Kast, J. Fan, N. Danilovic, S. W. Boettcher, *Chem. Mater*. **2015**, *27*, 8011ï 8020.

[7] a) C. C. L. McCrory, S. Jung, J. C. Peters, T. F. Jaramillo, *J. Am. Chem. Soc.* **2013**, *135*, 16977ï 16987; b) M. D. Merrill, R. C. Dougherty, *J. Phys. Chem. C* **2008**, *112*, 3655ï 3666.

[8] E. A. Kulp, S. J. Limmer, E. W. Bohannan, J. A. Switzer, *Solid State Ionics* **2007**, *178*, 749ï 757.

[9] M. S. Bruke, S. Zou, L. J. Enman, J. E. Kellon, C. A. Gabor, E. Pledger, S. W. Boettcher, *J. Phys. Chem. Lett*. **2015**, *6*, 3737ï 3742.

[10] T. D. Golden, A. Q. Wang, *J. Electrochem. Soc.* **2003**, *150*, C621ï C624.

[11] a) M. W. Louie, A. T. Bell *J. Am. Chem. Soc.* **2013**, *135*, 12329ï 12337; b) S. Klaus,Y. Cai, M. W. Louie, L. Trotochaud, A. T. Bell, *J. Phys. Chem. C* **2015**, *119*, 7243ï 7254.

[12] a) T. S. Sreeremya, K. M. Thulasi, A. Krishnan, S. Ghosh, *Ind. Eng. Chem. Res.* **2012**, *51*, 318ï 326; b) Z. Li, F. Han, X. Jiao, D. Chen, *RSC Adv.* **2016**, *6*, 60975ï 60982.

[13] a) J. Zhang, H. Wong, D. Yu, K. Kakushima, H. Iwai, *AIP Adv.* **2014**, *4*, 117117; b) L. Wang, F. Meng, *Mater. Res. Bull.* **2013**, *48*, 3492ï 3498; c) P. Singh, K. M. K. Srivastsa, A. Barvat, P. Pal, *Curr. Appl. Phys*. **2016**, *16*, 1388ï 1394.

[14] K. Zhao, J. Qi, H. Yin, Z. Wang, S. Zhao, X. Ma, J. Wan, L. Chang, Y. Gao, R. Yu, Z. Tang, *J. Mater. Chem. A* **2015**, *3*, 20465ï 20470.

[15] a) L. Trotochaud, S. L. Young, J. K. Ranney, S. W. Boettcher, *J. Am. Chem. Soc.* **2014**, *136*, 6744ï 6753; b) M. B. Stevens, C. D. M. Trang, L. J. Enman, J. Deng, S. W. Boettcher, *J. Am. Chem. Soc.* **2017**, *139*, 11361ï 11364; c) B. M. Hunter, W. Hieringer, J. R. Winkler, H. B. Gray, A. M. Müller, *Energy Environ. Sci.* **2016**, *9*, 1734ï 1743.

[16] a) P. Chakthranont, J. Kibsgaard, A. Gallo, J. Rak, M. Mitani, D. Sokaras, T. Kroll, R. Sinclair, M. B. Mogensen, T. F. Jaramillo, *ACS Catal.* **2017**, *7*, 5399ï 5409; b) C. G. Morales-Guio, L. Liardet, X. Hu, *J. Am. Chem. Soc.* **2016**, *138*, 8946ï 8957; c) M. E. G. Lyons, M. P. Brandon, *J. Electroanal. Chem.* **2009**, *631*, 62ï 70; d) S. B. Brachetti-Sibaja, M. A. Domínguez-Crespo, A. M. Torres-Huerta, W. De La Cruz-Hernández, E. Onofre-Bustamante, *J. Electrochem. Soc.* **2012**, *159*, C40ï C57.

[17] a) J. A. Haber, Y. Cai, S. Jung, C. Xiang, S. Mitrovic, J. Jin, A. T. Bell, J. M. Gregoire, *Energy Environ. Sci*. **2014**, *7*, 682ï 688; b) J. A. Haber, E. Anzenburg, J. Yano, C. Kisielowski, J. M. Gregoire, *Adv. Energy Mater.* **2015**, *5*, 1402307; c) M. Favaro, W. S. Drisdell, M. A. Marcus, J. M. Gregoire, E. J. Crumlin, J. A. Haber, J. Yano, *ACS Catal*. **2017**, *7*, 1248ï 1258.

[18] A. Ziani, T. Shinagawa, L. Stegenburga, K. Takanabe, *ACS Appl. Mater. Interfaces* **2016**, *8*, 32376-32384.

[19] A. Minguzzi, F.-R. F. Fan, A. Vertova, S. Rondinini, A. J. Bard, *Chem. Sci*. **2012**, *3*, 217-229.

[20] D. A. Lutterman, Y. Surendranath, D. G. Nocera, *J. Am. Chem. Soc.* **2009**, *131*, 3838-3839.

[21] a) D. R. Lide, *Handbook of Chemistry and Physics*, 84th ed.,CRC Press: Boca Raton, FL, **2003**; b) L. Hao, D. G. Leaist, *J. Chem. Eng. Data* **1996**, *41*, 210ï 213.

[22] a) M. Fleischmann, K. Korinek, D. Pletcher, *J. Chem. Soc., Perkin Trans.2*, **1972**, 1396ï 1403; b) M. A. A. Rahim, R. M. A. Hameed, M. W. Khalil, *J. Power Sources*, **2004**, *134*, 160ï 169; c) L. Ren, K. S. Hui, K. N. Hui, *J. Mater. Chem. A*, **2013**, *1*, 5689ï 5694.

[23] a) A. A. Keller, H. Wang, D. Zhou, H. S. Lenihan, G. Cherr, R. J. Cardinale, R. Miller, Z. Ji, *Environ. Sci. Technol.* **2010**, *44*, 1962ï 1967; b) M. Kosmulski, *Adv. Colloid Interfac.* **2009**, *152*, 14ï 25.

[24] M. Balasubramanian, C. A. Melendres, A. N. Mansour, *Thin Solid Films* **1999**, *347*, 178ï 183.

[25] F. Dionigi, T. Reier, Z. Pawolek, M. Gliech, P. Strasser, *ChemSusChem* **2016**, *9*, 962ï 972.

[26] T. Shinagawa, M. T.-K. Ng, K. Takanabe, *ChemSusChem* **2017**, *10*, 4155ï 4162.

10.1002/anie.201712121

WILEY-VCH

Entry for the Table of Contents

COMMUNICATION

Membrane coating for improved oxygen evolution stability. Highly durable oxygen evolution was successfully achieved by deposition of a CeO_x layer on electrocatalysts. The CeO_x layer has permselectivity, which suppresses the diffusion of redox ions while allowing OH^- and O_2 to permeate through. This permselectivity contributes to maintain the active sites underneath, resulting in excellent stability without changing the kinetics of the catalysts.

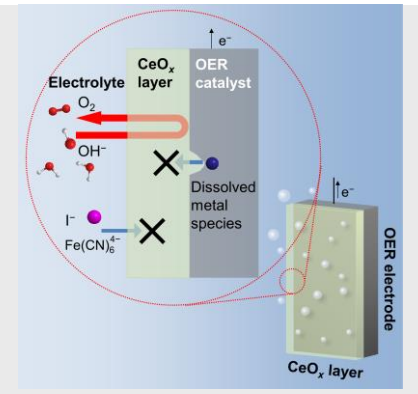

*Keisuke Obata, and Kazuhiro Takanabe**

Page No. – Page No.

A Permselective CeO_x Coating Improves the Stability of Oxygen Evolution Electrocatalysts